Surfaces and Interfaces 17 (2019) 100359

Contents lists available at ScienceDirect

Surfaces and Interfaces

journal homepage: www.elsevier.com/locate/surfin

# Biosynthesis of silver nanoparticles using bitter leave (*Veronica amygdalina)* *for* antibacterial activities

Samson O. Aisida[a,b], Kenneth Ugwu[c], Paul A. Akpa[d], Assumpta C. Nwanya[a,e,f], U. Nwankwo[a], Subelia S. Botha[g], Paul M. Ejikeme[h], Ishaq Ahmad[b,e,f], M. Maaza[e,f], Fabian I. Ezema[a,e,f,i,*]

[a] *Department of Physics and Astronomy, University of Nigeria, Nsukka, Nigeria*
[b] *National Centre for Physics, Quaid-i-Azam University campus, Islamabad 44000, Pakistan*
[c] *Department of Microbiology, University of Nigeria, Nsukka, Nigeria*
[d] *Department of Pharmaceutics, University of Nigeria, Nsukka, Nigeria*
[e] *Nanosciences African Network (NANOAFNET), iThemba LABS-National Research Foundation, 1 Old Faure road, Somerset West 7129, P.O. Box 722, Somerset West, Western Cape Province, South Africa*
[f] *UNESCO-UNISA Africa Chair in Nanosciences/Nanotechnology, College of Graduate Studies, University of South Africa (UNISA), Muckleneuk ridge, P.O. Box 392, Pretoria, South Africa*
[g] *Electron Microscope Unit, University of the Western Cape, South Africa*
[h] *Department of Pure and Industrial Chemistry, University of Nigeria, Nsukka, Nigeria*
[i] *Department of Physics, Faculty of Natural and Applied Sciences, Coal City University, Enugu, Nigeria*

ARTICLE INFO

*Keywords:*
Antibacterial
Biosynthesis
Nanoparticles
Bitter-leave
Nanomedicine

ABSTRACT

A green and facile biosynthesis of silver nanoparticles (SNPs) using dry Bitter leaves *(DBL)* (*Vernonia amygdalina)* aqueous extract as a capping and reducing agent was demonstrated in this work. The effect of the precursor's concentration on the size and shape of SNPs and its antibacterial activity is evaluated. The synthesized DBL_SNPs were characterized by using UV–visible spectroscopy, Fourier transforms infrared spectroscopy (FT-IR), X-ray diffraction (XRD), Scanning electron microscopy (SEM) and transmission electron microscopy (TEM). UV–visible spectra showed specific surface plasmon resonance absorption peak between 450 and 480 nm, which increases with the concentration confirmed the presence of nanoparticles. FTIR analysis revealed the presence of phytochemicals such as phenol, saponin, and alkaloid that play the major roles in stabilizing the synthesized DBL_SNPs. The TEM analysis showed the spherical shape of DBL_SNPs with the size ranges from 2 to 18 nm. XRD shows a crystallite fcc phase with broad peaks for sample a and crystal size of 22.4 nm, which decreases with higher concentrations. Antibacterial studies against Staphylococcus aureus and Coliform through diffusion method revealed 18.8 and 13.0 mm (for 80 μg/mL) inhibition zone for Coliform and Staphylococcus aureus respectively. The colloidal solution of DBL_SNPs formed was found to exhibit antibacterial activities against Coliform and Staphylococcus Aurea.

## 1. Introduction

Nanomedicine is a branch of nanotechnology in the scope of science that embodies biological, physical, and material sciences with serious impact in the therapeutic healthcare sectors [1,2]. This field possesses a promising way to improve the properties of metal for diverse applications by transforming them into nanoparticles with size ranges between 1 and 100 nm via eco-friendly synthetic. Inorganic metallic nanoparticles such as Silver, Gold, Zinc, Iron, Nickel, Platinum and their oxides have been given deep thought over the years through various syntheses. Among these, Silver nanoparticles have been harnessed thoroughly with applications in many areas of nanotechnology such as chemical sensing [3], catalysts in chemical reactions [4], Optical elements [5], pharmaceutical components [6] and antibacterial activity [7,8]. This metal via biosynthesis has paved the way for new antimicrobial agents against human pathogenic organisms due to excessive resistance of bacterial against antibiotic drugs [9], cosmetic and textile industries, water purification, and biomedical as a result of their unique characteristic such as biocompatibility and non-toxicity [1].

Metallic nanoparticles were previously prepared by various chemical and physical methods, such as electrochemical, microwave-assisted, and photochemical. Physical and chemical routes required high

* Corresponding author at: Department of Physics and Astronomy, University of Nigeria, Nsukka, Nigeria.
*E-mail addresses:* samson.aisida@unn.edu.ng (S.O. Aisida), fabian.ezema@unn.edu.ng (F.I. Ezema).

https://doi.org/10.1016/j.surfin.2019.100359
Received 6 June 2019; Received in revised form 12 July 2019; Accepted 21 July 2019
Available online 22 July 2019

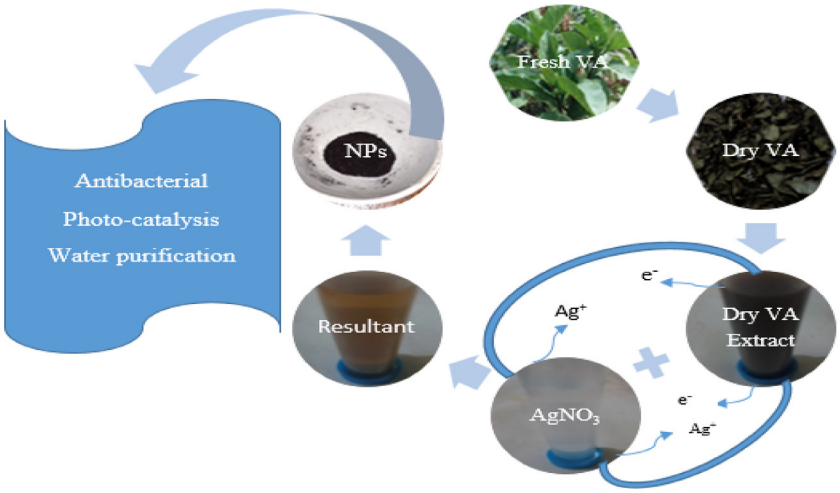


**Fig. 1.** Mechanism of formation of biosynthesis of DBL_SNPs.

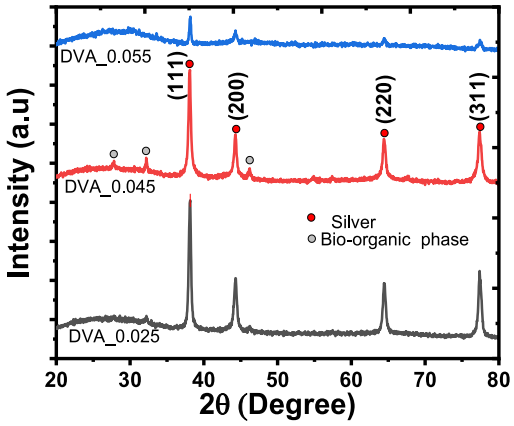


**Fig. 2.** XRD pattern of sample a, b and c.

energy and toxic chemicals that are expensive and difficult to scale up in large quantity [10,11,12]. As a result of these effects, biosynthesis of nanoparticles circumventing the aforementioned effects has been adopted recently to enhance the properties of the nanoparticles using micro-organism, animals' chitin, crude extract from the plant's leaves, seed and back. This method of synthesis is free of toxic, biocompatible, cost-effective, and eco-friendly [13,14].

Biosynthesis involve the use of green technology such as crude extracts from leaves of plants that are rich in metabolites such as flavonoid, alkaloid, tannin, saponin and phenolic acid that are responsible mainly for the reduction process of metal ion into bulk metallic nanoparticles formulation in the redox reaction to obtain nano-sized particle that are not toxic by converting $Ag^{+}$ *to* $Ag^{0}$ and also serve as the capping agent of the biosynthesized nanoparticles [10,11,15–20]. Bitter leaf (BL) is a shrub of about 2–5 m high popularly found in Africa continent. It has a green leave with a bitter taste [21]. It is often referred to as a medicinal plant because of its therapeutic and prophylactic properties which are widely used for the prevention, treatment of disease, and symptom relief [22]. Dry bitter leaves (DBL) has high turbidity, and low pH compared with the fresh BL. DBL is very rich in phytochemicals such as alkaloid, tannins, saponins, flavonoids, and a steroid which can function as metal reducing as well as a capping agent on the metal nanoparticles in a single route [22]. The bitter taste of the DBL is as a result of the anti-nutritional factors, such as alkaloid, saponins, and tannins [23].

This work aid the biosynthesis of silver nanoparticles using bitter leaves (*Vernonia amygdalina)* as a reducing and capping agent. The antibacterial activities of DBL_SNPs were investigated for the first time against Gram-positive *Staphylococcus aureus* and gram-negative *Coliform*. The DBL_SNPs shows an auspicious antibacterial agent.

## 2. Materials and methods

### 2.1. Materials

All the reagents were of analytical grade and used as received without further purification. Anhydrous silver nitrate ($AgNO_3$) (99.8%), Muller-Hinton agar, swab stick, Muller-Hinton broth, and Gentamycin were obtained from Sigma Aldrich (Germany). Gram-positive bacterial strain *Staphylococcus aureus* and gram-negative strain Coliform were obtained from Classic biomedical laboratory, University of Nigeria, Nsukka. Fresh bitter leaves were collected from the earth. The taxonomic verification was done at the Department of Plant Science, University of Nigeria, Nsukka. All the aqueous solutions were prepared using distilled water (DW).

### 2.2. Collection and preparation of dry bitter leaves (DBL)

100 g weight of the fresh leaves of GL was thoroughly washed with distilled water (DW) to remove debris and dust particles. The clean leaves are then incised into pieces and dry on a white formica board under room temperature for 72 h The DBL was then crushed into powder and 10 g was dissolved in 500 mL DW followed by heating at 80 °C for 1 h, after which the system is allowed to cool to room temperature. The mixture was filtered using a sieve followed by a filter cloth and Whitman No.1 filter paper. The filtrate is decanted and preserved in a refrigerator at a temperature of 4 °C for further usage. The following phytochemicals (flavonoid, phenol, and tannins) were present in the extract in large quantities, among others.

### 2.3. Biosynthesis of silver nanoparticles by dry bitter leaves (DBL)

Three concentrations ranging between 0.025, 0.045 and 0.055 g of $AgNO_3$ crystals were dissolved in 100 mL of DW followed by continuing stirring for 1 h using a magnetic stirrer to ensure uniform dissolution. 50 mL of DBL extract was then added dropwise to 50 mL of $AgNO_3$ solution in the ratio 1:1 to form an equal volume mixture for each concentration while stirring at room temperature for another 2 h to form a homogeneous solution. The homogeneous solution was centrifuged at 1500 ppm for 30 s and the obtained dry bitter leaves silver nanoparticles ((DBL_SNPs (as shown in Fig. 1) were washed six (6) times with DW and dried in a hot air oven for further characterization. The three concentration formed nanoparticles were label as sample a, b

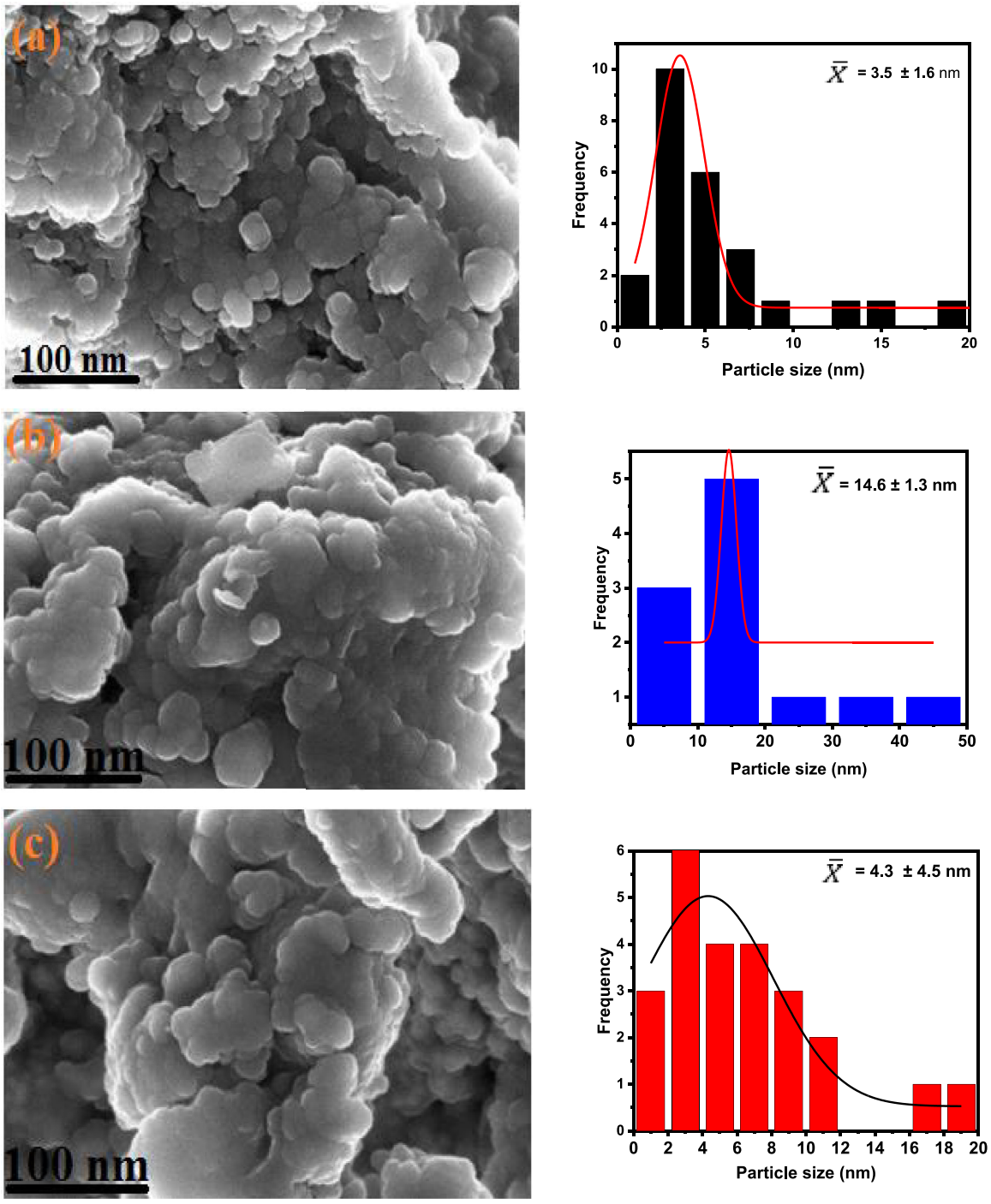


**Fig. 3.** SEM images, EDX, and size distribution histogram for sample a, b and c.

and c. The biosynthesis enhanced the reduction of $Ag^+$ ions to $Ag^0$ atoms from the supernatant of the enzymatic extracts of BL as shown in Eq. (1).

$$Ag^+ + e - (phytochemicals enzymes) \rightarrow Ag^0 \quad (1)$$

## 3. Result and discussion

The structural studies of sample a, b and c formed from the three concentrations of DBL_SNPs were studied using the Shimadzu-7000 powder X-ray diffractometer with Cu-Kα radiation (λ = 1.5406 Å) and lattice parameter ($a$ = 4.08620 Å) at room temperature in the continuous scanning mode and a scanning 2θ range of 15°–80° The surface morphologies of the samples were obtained using a field emission high-resolution scanning electron microscope (Auriga Zeiss HRSEM). Transmission electron microscopy (TEM) micrographs, selected area electron diffraction (SAED) patterns, and high-resolution transmission electron microscopy (HRTEM) images were obtained using a Tecnai F20 High-Resolution Transmission Electron Microscope (HRTEM) operated at 200 kV, equipped with an Energy Dispersive X-ray Spectrometer (EDS) for elemental analysis. Selected-area electron diffraction (SAED) (IH-300X). A Perkin Elmer Fourier transforms infrared spectrophotometer (FTIR) was used for the determination of the surface functional groups. The elemental composition was determined using the selected area electron diffraction (SAED) (IH-300X) analysis. Also, the absorption was determined by UV–vis spectrophotometer (UV-

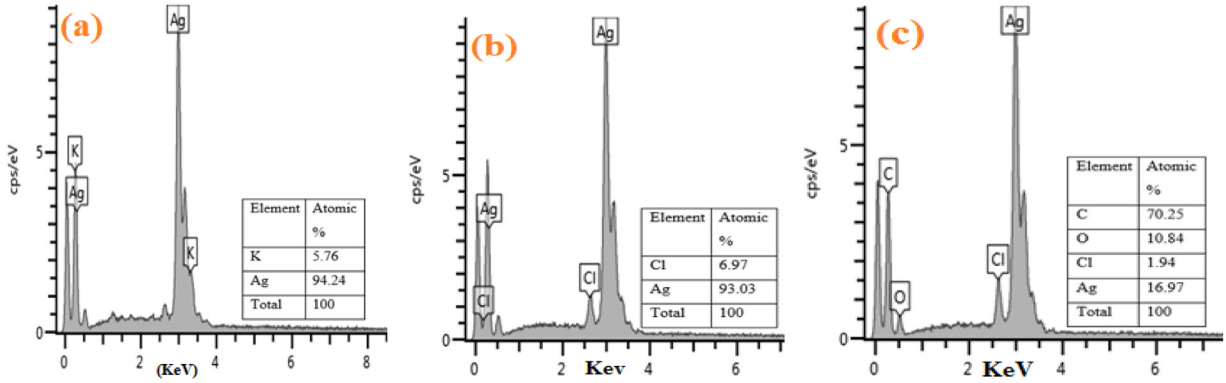


**Fig. 3.** (*continued*)

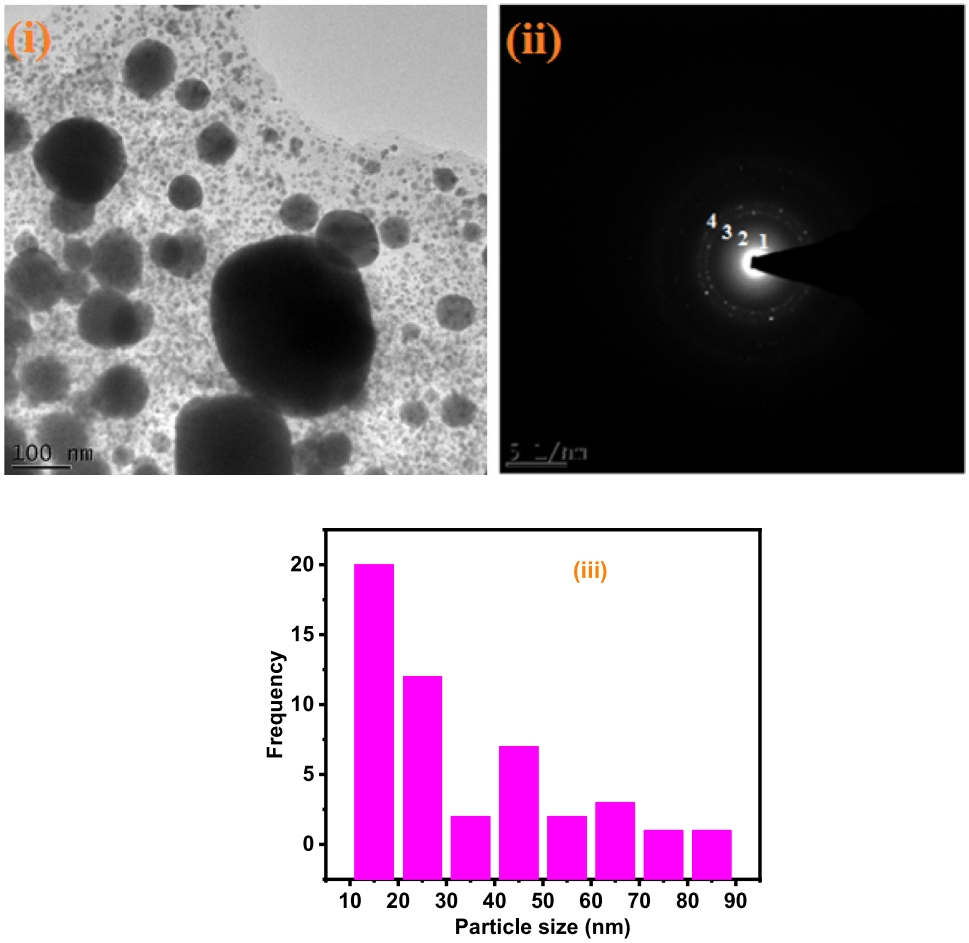


**Fig. 4.** TEM micrograph of sample a.

7504) in the wavelength range of 200–1000 nm.

### 3.1. XRD analysis of DBL_SNPs

The XRD analysis, as shown in Fig. 2 was used to determine the phase purity and the crystallinity of DBL_SNPs for the three concentrations. The peaks observed at2θ values of 38.05°, 44.33°, 64.43°, 77.46° with JCPD No: 04–0783 could be corresponding to the crystallographic planes (111), (200), (220) and (311) of the DBL_SNPs with face-centered cubic silver lattice. The particle crystallite size of 22.4, 21.4, and 17.9 nm was obtained for sample a, b and c respectively using Scherer formula in Eq. (2). The broadest peak at the plane (111) was observed to decrease as the concentration of the precursor increases.

$$D = \frac{0.9\lambda}{\beta \cos\theta} \quad (2)$$

where *D*is the crystallite size (nm), λ is the X-ray wavelength (λ = 1.5406 Å), β is the full width at half maximum (FWHM) of the diffraction peaks measured in radians and θ is the Bragg diffraction angle [24].

### 3.2. SEM analysis of DBL-SNPs

Fig. 3 gives the surface morphology and the size distribution of the biosynthesized samples. The images give spherical shape particle size between 5 and 20 nm for all the concentrations with a compact grain of different shapes for sample a with an average size of 3.5 nm, highly

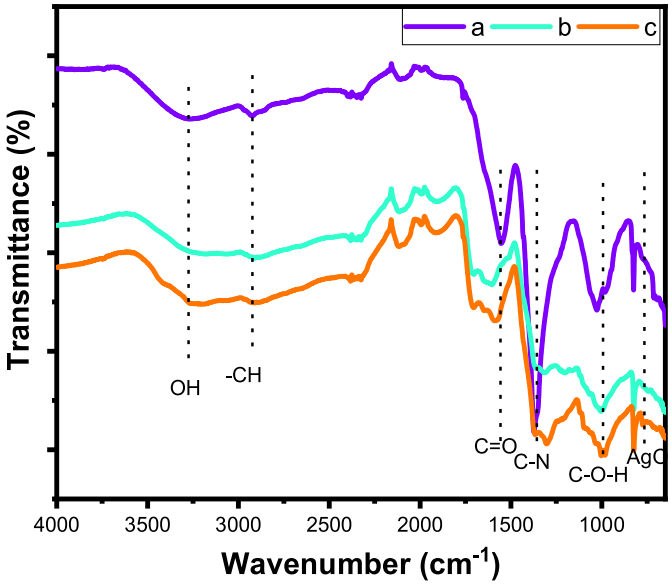


**Fig. 5.** FTIR graph of sample a, b and c.

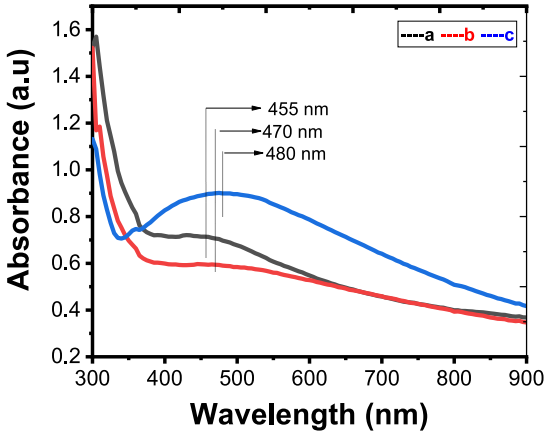


**Fig. 6.** UV–Visible absorption spectra of sample a, b and c.

**Table 1**
Zone of inhibition of DBL_NPs and Ciprofloxacin.

| | Inhibition zone (mm) | | | | |
|---|---|---|---|---|---|
| **Organisms** | **D0** | **D1** | **D2** | **D3** | **Cipro.** |
| **S. Aureus** | **0.0** | **10.0** | **11.0** | **13.0** | **24.9** |
| **Coliform** | **0.0** | **10.2** | **12.3** | **18.8** | **28.0** |

Do = DW, D1–D3 are the doses of DBL_NPs and Cipro. = Ciprofloxacin.

aggregated spherical grains for sample b and an average size of 14.6 nm and aggregated spherical grains for sample c with an average size of 4.3 nm. The Energy Dispersive X-ray diffraction (EDX) as shown in Fig. 3 shows all the elements present in the compound. The EDX elemental analysis confirmed the desired composition of all elements with sample a having the highest peak for silver at 94.24%; this decreases to 16.97% for sample c

### 3.3. TEM and SAED analysis of DBL_SNPs

The TEM micrograph given in Fig. 4i shows that the particles were predominantly spherical in shape without aggregation; this is an indication of good stabilization of the NPs via DBL. The inset shows the size distribution histograms estimated over 100 particles, and the majority of the particle was found to be between 5 and 25 nm in agreement with the XRD value. The SAED, as shown in Fig. 4ii, shows the polycrystallinity of the samples with several sharp rings; this confirmed that the formulated nanostructure is highly polycrystalline in nature. The formed rings 1, 2, 3, 4 may be attributed to the diffraction from (1 1 1), (2 0 0), (2 2 0) and (3 1 1) planes of a face-centered cubic (fcc).

### 3.4. FTIR Spectra analysis of DBL_SNPs

The interactions between the chemical moieties present in *DBL_SNPs* formulated were analyzed by FTIR spectroscopy, which revealed the two main vibrations (i.e. stretching and bending) in the wavelength range of 4000–500 $cm^{-1}$ as shown in Fig. 5. The peak at 3281 $cm^{-1}$ is due to (−OH stretching) [25–27], 2924 $cm^{-1}$ corresponding to (−CH stretching, alkanes group), 1566 $cm^{-1}$ (C═O, carbonyl group), the band at 1364 $cm^{-1}$ is associated with C−N stretching vibration of aromatic amines showing the presence of water-soluble caffeine. 993 $cm^{-1}$ (−C−O−C phenolic hydroxyl group). The organic functional groups on the surface of the synthesized DBL_SNPs indicate the interaction between silver nitrate and DBL. The reduction of silver ions to metallic silver, arose due to the strong affinity of the bioactive compounds in DBL towards the silver ions to donate free electrons. Moreover, the peak at 682 $cm^{-1}$ can be attributed to AgO bond, suggesting the birth of DBL_SNPs [28–30]. The obtained results is in conformity with the previous research work [31,32].

### 3.5. UV–Visible spectral analysis of DBL_SNPs

The absorbance of sample a, b and c as shown in Fig. 6 was observed with the color change due to the reduction of pure silver metal ions to Ag-NPs via the reactive functional moieties present in DBL. The colour change was observed to change to dark brown after the reaction as a result of the excitation between the precursor and the reducing agent given the Surface Plasmon Resonance (SPR) peak at 455, 470 and 475 nm respectively for the three samples within the visible range (390–490 nm) [33–35]. The results obtained are in agreement with the previous work [36,37]. The SPR increases with the concentration of the precursor.

### 3.6. Antibacterial assay of DBL_SNPs

A modified Ager Well-Diffusion Method (AWDM) was used to analyze the antibacterial activity of DBL_NPs against *Staphylococcus aureus* (Gram-positive) *and Coliform* (Gram-negative) [25,28,38,39]. Mueller Hinton Agar (MHA) was dissolved in DW and stirred vigorously to obtain a homogenous solution. The homogeneous solution was autoclaved for about 30 min, after which 20 mL of the autoclaved mixture was dripped in each of the sterilized Petri plates and allowed to jell for 1 h. The freshly stock cultures of Staphylococcus aureus and coliform isolates of ≈ $10^6$CFU/mL prepared in nutrient broth were smeared on the MHA plates. The DBL_SNPs obtained was tested against the bacteria organism. Five h broth cultures of the obtained bacteria were applied on the surface of the nutrient agar using a swab stick. A sterile flamed cork borer of 8 mm diameter size was used to drill wells in each of the seeded plates and 20, 50, 80, µLdoses of this test solution containing 0.2, 0.5 and 0.8 mg were dispensed in each well respectively. The agar plates were then left to stay for 1 h at room temperature and finally, the plates were incubated for 24 h at 37 °C in an incubator. Standard antibiotic drug *ciprofloxacin* was used as the positive control and distilled water as a negative control; both were tested against the pathogens. The size of the inhibition zone was measured, and the mean value for each organism was recorded and expressed in millimeter (mm) (as shown in Table 1). The formulated DBL_SNPs was found to show momentous bactericidal against the bacterial strains, as shown in Fig. 7. It was observed from Fig. 8, the susceptibility of DBL_NPs against the pathogens increases as the doses increases through the inhibition zone, and it was higher for Coliform organism. This increase in the strength of

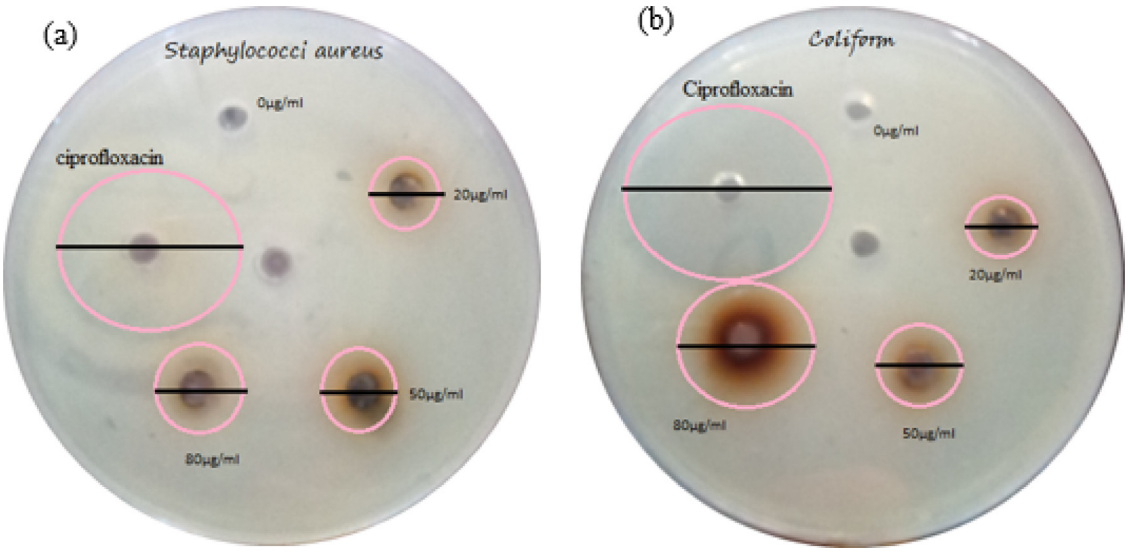


**Fig. 7.** Antibacterial activities of DBL_NPs against (a) *Staphylococcus aureus* and (b) *Coliform*.

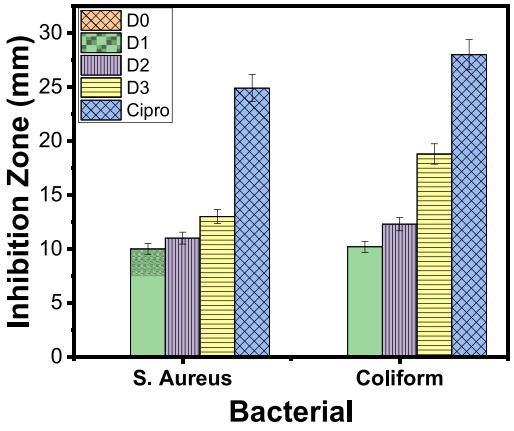


**Fig. 8.** Antibacterial activities of synthesized DBL_NPs against human pathogens.

DBL_NPs shows that DBL_NPs is viable for antibacterial activities, especially for the Coliform organism.

## 4. Conclusion

Biosynthesis of DBL_NPs from bitter leaves *(Vernonia amygdalina)* extract is the latest alternative to a chemical and physical synthesis sequel to its novel toxicity free, eco-friendly and biocompatibility. This work reported the synthesis of silver nanoparticles using DBL which provide a simple, reliable, and eco-friendly way of synthesizing nanoparticles. The reduction of silver ion to silver atom was observed by UV visible with SPR peak in the range of 450–480 nm. The XRD analysis confirmed the highest peak of DBL_NPs crystal correspond to (111) diffraction plane. The SEM confirmed a spherical morphology for all the concentrations. The FTIR study shows the metabolites in DBL responsible for its bio-reduction. The FTIR study suggests that the protein in the extract might play an important role in the stabilization of silver. The formulated DBL_NPs is auspicious as an antibacterial agent against multidrug-resistant bacterial strains.

## Conflict of interest

We declare there is no conflict of interest.

## Acknowledgments

Samson O. Aisida appreciates the NCP-TWAS Postdoc fellowship (NCP-CAAD/TWAS_Fellow8408). ACN (90406558) and FIE (90407830) cordially acknowledge UNISA for Postdoc and VRSP Fellowship awards, respectively. We graciously acknowledge the grant for this project by TETFUND under Institutional Base Research (IBR). We thank the US Army Research Laboratory–Broad Agency Announcement (BAA) for the financial support given to this research. Also, we thank Engr. Emeka Okwuosa for the generous sponsorship of April 2014, July 2016 and July 2018 conference/workshops on applications of nanotechnology to energy, health & Environment conference and for providing some research facilities.

## References

[1] P. Saba, G. Maryam, B. Saeid, Mater. Sci. Eng. C 98 (2019) 250–255.
[2] A. Syed, S. Saraswati, G. Kundu, A. Ahmad, Spectrochimica Acta Part A 114 (2013) 144–147.
[3] W. Songping, M. Shuyuan, Mater. Chem. Phys. 89 (2005) 423–427.
[4] Z.J. Jiang, C.Y. Liu, L.W. Sun, J. Phys. Chem. B 109 (2005) 1730–1735.
[5] J.M. Nam, S.J. Park, C.A. Mirkin, JACS 124 (2002) 3820–3821.
[6] C. Aymonier, U. Schlotterbeck, L. Antonietti, P. Zacharias, R. Thomann, J. Tiller, S. Mecking, Chem. Commun. 2002 (2010) 9–21.
[7] V. Dhand, L. Soumya, S. Bharadwaj, S. Chakra, D. Bhatt, B. Sreedhar, Mater. Sci. Eng. C 58 (2016) 36–43.
[8] B. Ajitha, Y.K. Ashok, P.S. Reddy, Acta Mol. Biomol. Spectrosc. 121 (2014) 164–172.
[9] J.H. Mohammad, M.F. Katharina, A.A. Ali, J.D. Dorleta, R.D. Idoia, R. Teofilo, M. Morteza, Trends Biotechnol. 10 (2012) 1016.
[10] R. Tahir, B. Muhammad, M.I. Hafiz, L. Chuanlong, Colloids Surf. B 158 (2017) 408–415.
[11] S.V. Ravichandran, S. Sivadasan, A.A. Syed, H. Rajak, Mater. Lett. 180 (2016) 264–267.
[12] M. Mastuli, R. Rusdi, A. Mahat, N. Saat, N. Kamarulzaman, Adv. Mater. *Res.* 545 (2012) 137–142.
[13] S. Ouda, Res. J. Microbiol. 9 (2014) 34–42.
[14] P. Singh, R. Raja, Asian J. Exp. Biol. Sci. 2 (2011) 600–605.
[15] D. Manoja, S.S. Soumya, Appl. Nanosci. 8 (2018) 1059–1067.
[16] P. Azmath, S. Baker, D. Rakshith, S. Satish, Saudi Pharm. J. 24 (2015) 140–146.
[17] V. Arya, Dig. J. Nanomater. Biostruct. 5 (2010) 9–21.
[18] C. Krishnaraj, P. Muthukumaran, R. Ramachandran, M. Balakumaran, P. Kalaichelvan, Biotechnol. Rep. 4 (2014) 42–49.
[19] N.M. Shinde, A.C. Lokhande, J.S. Bagi, C.D. Lokhande, Mater. Sci. Semicond. Process. 22 (2014) 28–36.
[20] N.M. Shinde, A.C. Lokhande, C.D. Lokhande, J. Photochem. Photobiol. B 136 (2014) 19–25.
[21] N. Yakubu, A. O.Amuzat, R.U. Hamzat, Am. J. Food. Nutr. 2 (2012) 26–30.
[22] G. Igile, W. Oleszek, R. Aquino, D. Vernonisides, J. Natl. Prod. 58 (1995) 438–443.
[23] G. Oboh, Wiss. *U-Technol.* 38 (2005) 513–517.
[24] B. Cullity, Element of X-ray Diffraction, second ed., Addison-Wesley, London, 1978.
[25] G. Manjul, J. n. Geeta, Int. J. Biomater. (2018), https://doi.org/10.1155/2018/

6735426.
[26] J.Y. Song, H.-.K. Jang, B.S. Kim, Process. Biochem. 44 (2009) 1133–1138.
[27] H. Susanto, Y.U. Feng, J. Food Eng. 91 (2009) 333–340.
[28] S.O. Aisida, N. Madubuonu, M. Hisham Alnasir, I. Ahmad, S. Botha, M. Maaza, F.I. Ezema, Appl. Nanosci. (2019), https://doi.org/10.1007/s13204-019-01099-x.
[29] K. Kombaiah, J.V. Judith, L.K. John, M. Bououdina, R.R. Jothi, A.A.-l Hamad, Mater. Chem. Phys. 204 (2018) 410–419.
[30] C. Ladole, Int. J. Chem. Sci. 10 (2012) 1230.
[31] D. Kumar, G. Kumar, V. Agrawal, Parasitol. Res. 117 (2018) 377–389.
[32] R.R. Wallace, T.P. Milena, D.A. Bruna, S.F. Letícia, N.C. Fanny, S.B. Juliana, ... B.S. Amedea, Appl. Surf. Sci. 463 (2019) 66–74.
[33] H. Obayashi, K. Nakano, H. Shigeta, M. Yamaguchi, K. Yoshimori, M. Fukui, ... M. Kondo, Biochem. Biophys. Res. Commun. 226 (1996) 37–41.
[34] M.A. Jalaluddin, A.A. Mohammad, M.K. Haris, A.A. Mohammad, C. Inho, Sci. Rep. 6 (2016) 20414.
[35] B. Mahmoodreza, H.P. Ayat, N. Ali, Z. Masood, M. Roya, M. Aliyar, Int. J. Biol. Macromol. 124 (2019) 148–154.
[36] S.J. Jacob, J. Finub, A. Narayanan, Colloids Surf. B 91 (2012) 212–214.
[37] P. Singh, K. Bhardwaj, P. Dubey, A. Prabhune, RSC Adv. 5 (2015) 24513–24520.
[38] P.R. Murray, E.J. Baron, M.A. Pfaller, F.C. Tenover, R.H. Yolke, Manual of Clinical Microbiology 6 ASM, Washington, DC, 1995.
[39] R.P. Samy, S. Ignacimuthu, J. Ethnopharmacol. 69 (2000) 63–71.